FLUKA simulations of energy density deposition from a ILC bunch in different spoiler designs

L. Fernandez-Hernando[1], N.K.Watson[2]

March 20, 2006

Abstract

FLUKA is used to simulate the energy deposition due to a direct bunch impact of the ILC beam in various candidate spoiler designs. The conclusions extracted will contribute to the overall optimisation process and identify areas where additional experimental data would be beneficial.

[1] CCLRC, Daresbury Laboratory, UK
[2] School of Physics and Astronomy, Univ. of Birmingham, Birmingham, UK

1 Introduction

Due to the impossibility of actually testing candidate ILC spoilers in the exact same beam conditions of size and energy as the ILC, it is necessary to rely heavily on simulation for a large part of the process of optimising the spoiler jaws. Simulations of both energy deposition via electromagnetic processes, and of the resulting mechanical stresses caused by the rapid heating of the material, need to be considered. This report describes predictions for energy deposition and corresponding temperature rises in a variety of different spoiler jaw configurations, obtained using the FLUKA Monte Carlo [1,2]. The results can be compared with those obtained using other physics Monte Carlos [3], and used as input to ANSYS modelling of the impact on the bulk material properties [4]. These studies form part of the R&D for spoiler material optimisation referred to in the ILC Baseline Configuration Document (BCD) for the Beam Delivery System [5].

Different options, such as a full metal spoiler using either titanium, titanium alloy Ti-6Al-4V (90% Ti, 6% Al, 4% V) or aluminium, and different combinations of graphite and alloy have been simulated. Metal is necessary in order to have the high electrical conductivity that will help to suppress the electric wakefields generated by the electrons in the bunch. Although titanium has lower electrical conductivity than copper, its higher melting point (~1941K versus the 1358K of copper) make it a more suitable candidate to survive the temperature increases generated by the impact of one or more bunches. Aluminium also shows a rather low melting point compared to titanium (933.47 K), but its larger radiation length (8.9 cm against 3.56 cm of titanium) avoids an energy deposition as high as with the other metals.

In the ILC BCD [5], spoilers are defined to be between 0.5 and 1.0 radiation lengths thick, to ensure appropriately lowered energy density incident on the downstream absorbers. They are also required to be "survivable", i.e. not be damaged, either by melting of their material or fracture, by 2 (1) bunches at 250 (500) GeV. It is desirable to have short spoilers that do not take up large amounts of space along the beamline, but this must be balanced with the requirement to avoid rapid changes in aperture which lead to large geometric contributions to the transverse wakefields. To reduce the transverse wakefield component a smooth transition between the aperture of the beam pipe to the narrowest aperture of the spoiler jaws is recommended. This leads to designs consisting of two tapers, a leading taper (wedge) upstream of the main body of the spoiler and a trailing taper downstream. As the optimisation of the external geometry of the spoiler (taper angle) for wakefields is still in progress [6], a taper angle of 335mrad has been used arbitrarily throughout, motivated by the fact that this corresponds to one of the insertions to be used in the T-480 run at SLAC in Apr/May 2006.

To achieve reasonable longitudinal dimensions of the spoiler, it is assumed that most of the required radiation length be in the form of metal, e.g. Cu. The strong dependence of the number of radiation lengths traversed by a beam entering a tapered spoiler on the displacement from the beam axis, make it attractive to consider using a long radiation length material as a bulk, covered by a thin layer of metal, rather than a homogeneous metal spoiler.

This extra material makes it interesting to consider a range of options, incorporating metals and graphite. In the following sections several of these options are presented together with the predictions for impact by a bunch of $2 \cdot 10^{10}$ electrons at 250 GeV, with beam size of σ_x=111 μm and σ_y=9 μm, and at 500 GeV, with σ_x=79.5 μm and σ_y=6.36 μm [7]. These studies can be extended for different machine configurations in the future, such as Low Q configuration [8] which presents the lowest beam size in the collimator position.

2 Different spoiler options and results

For all the different options four different simulations have been generated with an arbitrary choice of depths to illustrate that the extent to which the beam is mis-steered has implications for tapered spoilers: with the beam colliding 2 mm deep from the top of the spoiler at 250 GeV and at 500 GeV, and with the beam 10 mm from the top at 250 GeV and 500 GeV as well as shown in figure 1.

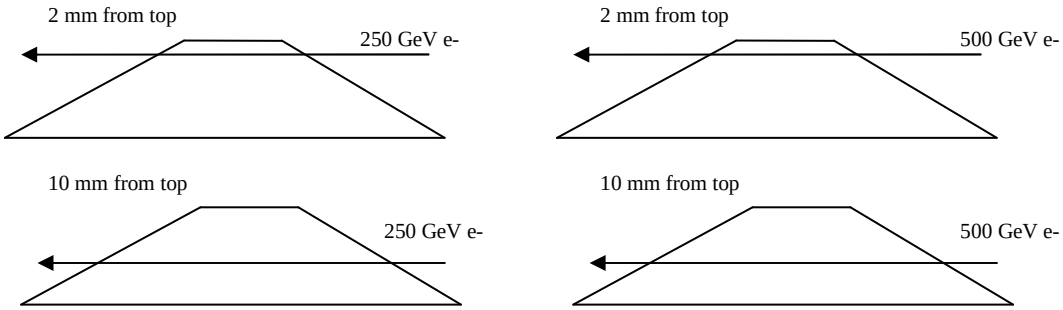

Figure 1. Four different tests.

2.1 Full metal spoilers

Four full metal spoilers have been simulated: a full titanium body, a full titanium alloy body (90% Ti, 6% Al, 4% V), a full aluminium one and a copper one. Results from the simulations are presented in the following sections.

2.1.1 Full titanium alloy spoiler

Dimensions for this spoiler can be seen at figure 2, with visualisation performed using the SimpleGeo tool [9].

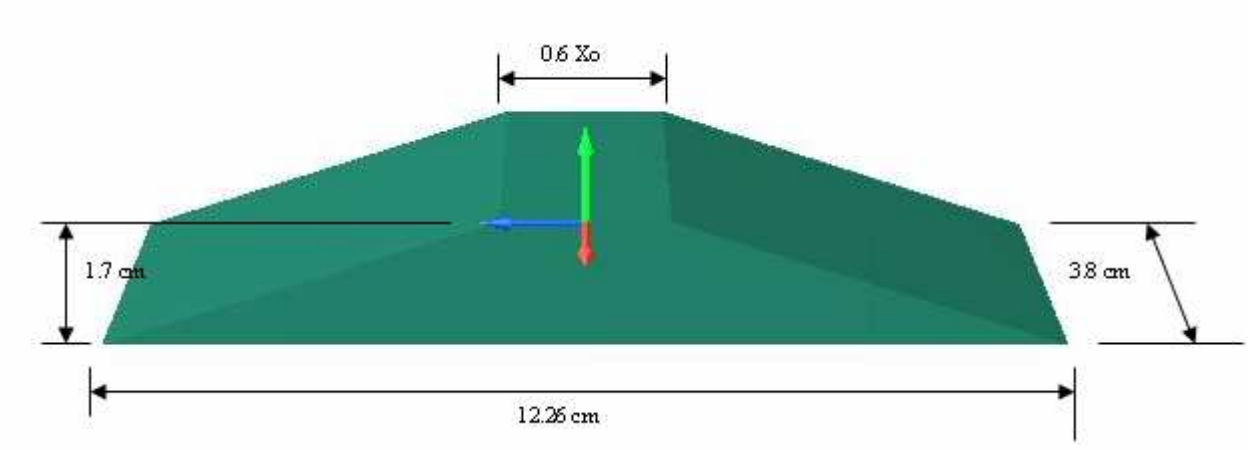

Figure 2. Full Ti-alloy spoiler, visualised using SimpleGeo [9].

The following plots at figure 3 represent the temperature increase after a bunch of $2 \cdot 10^{10}$ electrons at 250 GeV (left plots) and at 500 GeV (right plots) in the beam region, for a

volume of 10 µm in x (horizontal), 2 µm in y (vertical) and along all the z (beam). It can be observed how the increase of temperature is higher at the exit of the spoiler than at the start of it. The incident electrons generate an electromagnetic shower that increases along the entire path thus depositing more energy in the material and increasing its temperature.

Table 1 lists the maximum temperature for each of the four cases. Notice the difference of top temperature achieved if the bunch traverses 5 cm more material, as in the case of the beam hitting 10 mm deep from the top of the spoiler. In two cases, 500 GeV energy 2 mm from top and 250 GeV energy 10 mm from top, the material reaches a temperature high enough to fracture or crack. In the case of 500 GeV energy 10 mm from top the temperature is high enough to melt the alloy.

An earlier simulation showed that the increase in temperature is around a 10% higher when using pure titanium instead of the alloy.

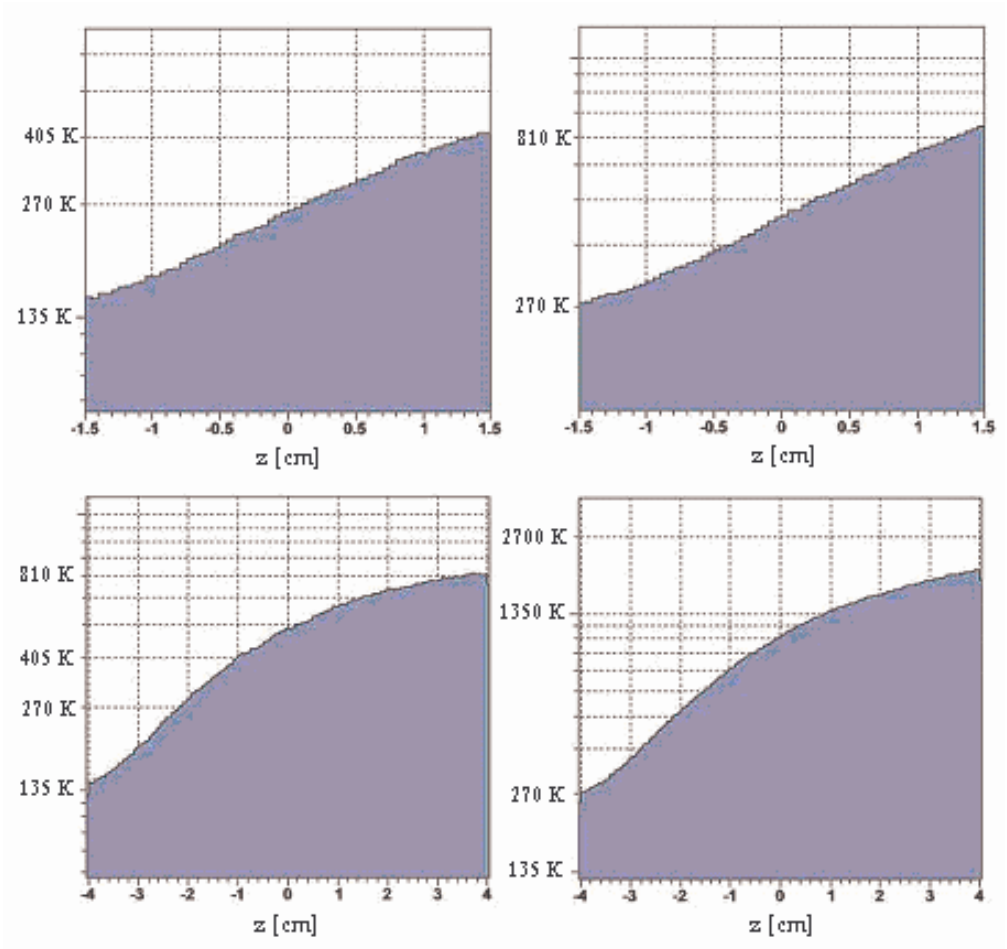

Figure 3. Temperature rises, extracted using FlukaGUI [10] for a full Ti alloy spoiler.

Table 1. Top temperatures in all four cases for a full Ti alloy spoiler.

	ΔT [K]; 250 GeV e^-	ΔT [K]; 500 GeV e^-
2 mm from top	420	870
10 mm from top	850	2000
Difference	102%	130%

2.1.2 Full aluminium spoiler

The aluminium spoiler is around 3 cm longer than the titanium or titanium alloy one (dimensions are shown in figure 4) due to its longer radiation length but this also leads to a smaller energy deposition in the material, as can be observed in the plots from figure 5.

The increases of energy are not as high as in the full titanium case however. Taking into account that these spoilers could work at room temperature, the melting temperature is reached in the case of 500 GeV energy 10 mm from top. The situation is less clear for the fracture temperature, but if it is assumed to be approximately half of the melting temperature (around 420-460 K) then metal reaches fracture temperature in the remaining cases.

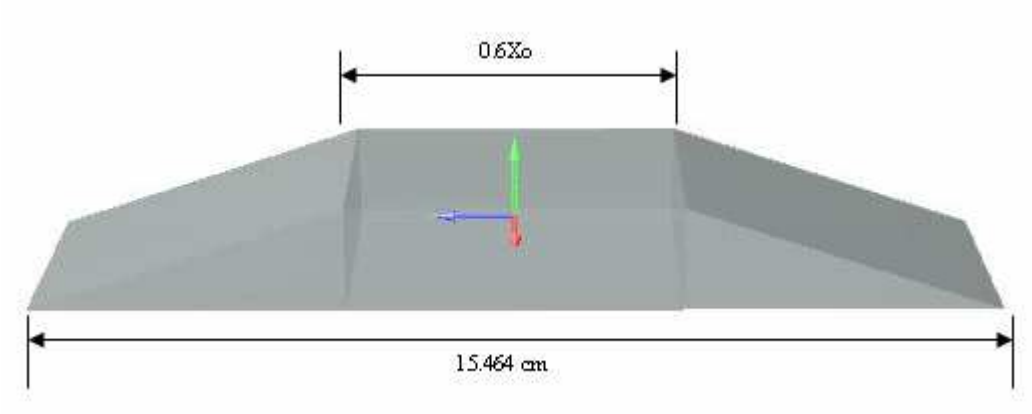

Figure 4. Aluminium spoiler.

Table 2. Top temperatures in all four cases for a full Al spoiler.

	ΔT [K]; 250 GeV e^-	ΔT [K]; 500 GeV e^-
2 mm from top	200	410
10 mm from top	265	595
Difference	33%	45%

Table 2 lists the top temperature increases for the aluminium spoiler. Difference between the 2 mm and 10 mm cases are more moderate, partly due to the fact that the difference in the path length traversed by the beam is not as large as with the titanium spoiler.

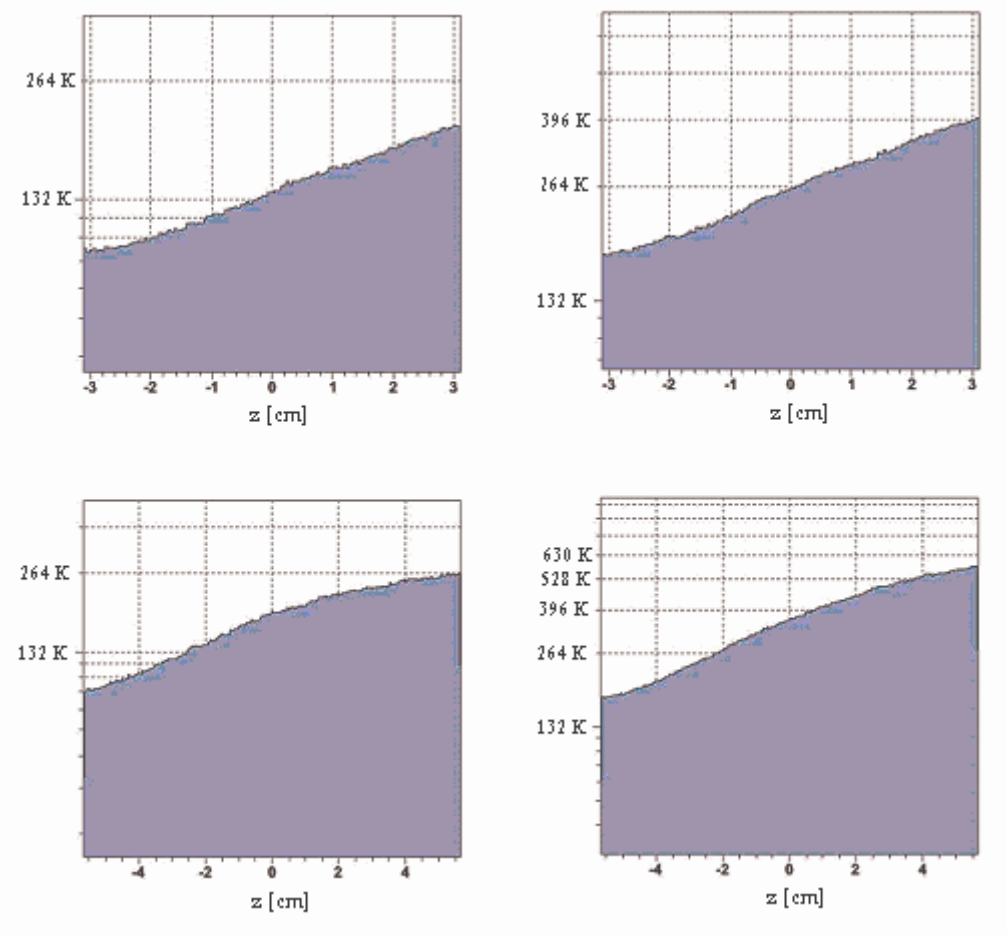

Figure 5. Temperature rises for a full Al spoiler.

2.1.3 Full copper spoiler

The copper spoiler has the advantage from the point of view of wakefields that is has the highest electrical conductivity. It is also shorter (almost 1.3 cm shorter than the titanium spoiler and 3.3 cm shorter than the aluminium one), therefore is the best option to reduce resistive wakefields. Its main disadvantage is the short radiation length of copper that could be translated into a high energy deposition when a electron bunch hits it in. Figure 6 shows a picture of this spoiler and figure 7 the peak temperature increases along z.

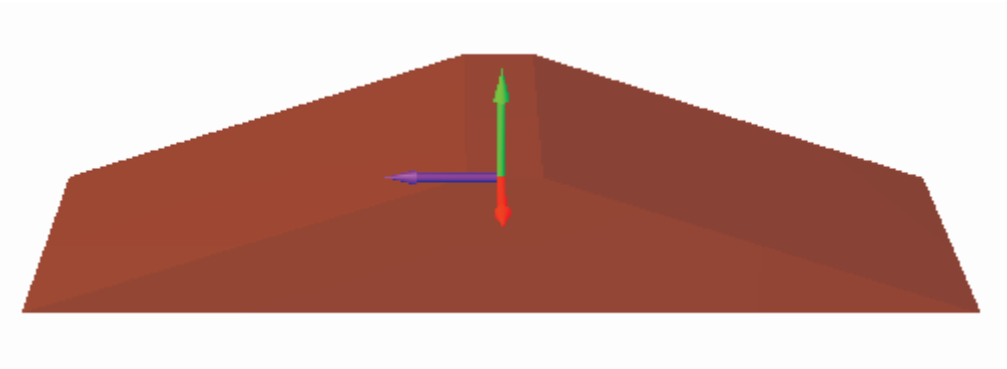

Figure 6. Copper spoiler.

Table 3 shows the top temperatures achieved at each case. Melting temperature for copper is around 1360 K and this temperature is reached in all four cases, showing clearly how inadequate copper is as collimator material in case of errant beam incident.

Table 3. Top temperatures in all four cases for a full Cu spoiler.

	ΔT [K]; 250 GeV e^-	ΔT [K]; 500 GeV e^-
2 mm from top	1300	2700
10 mm from top	2800	7000
Difference	115%	159%

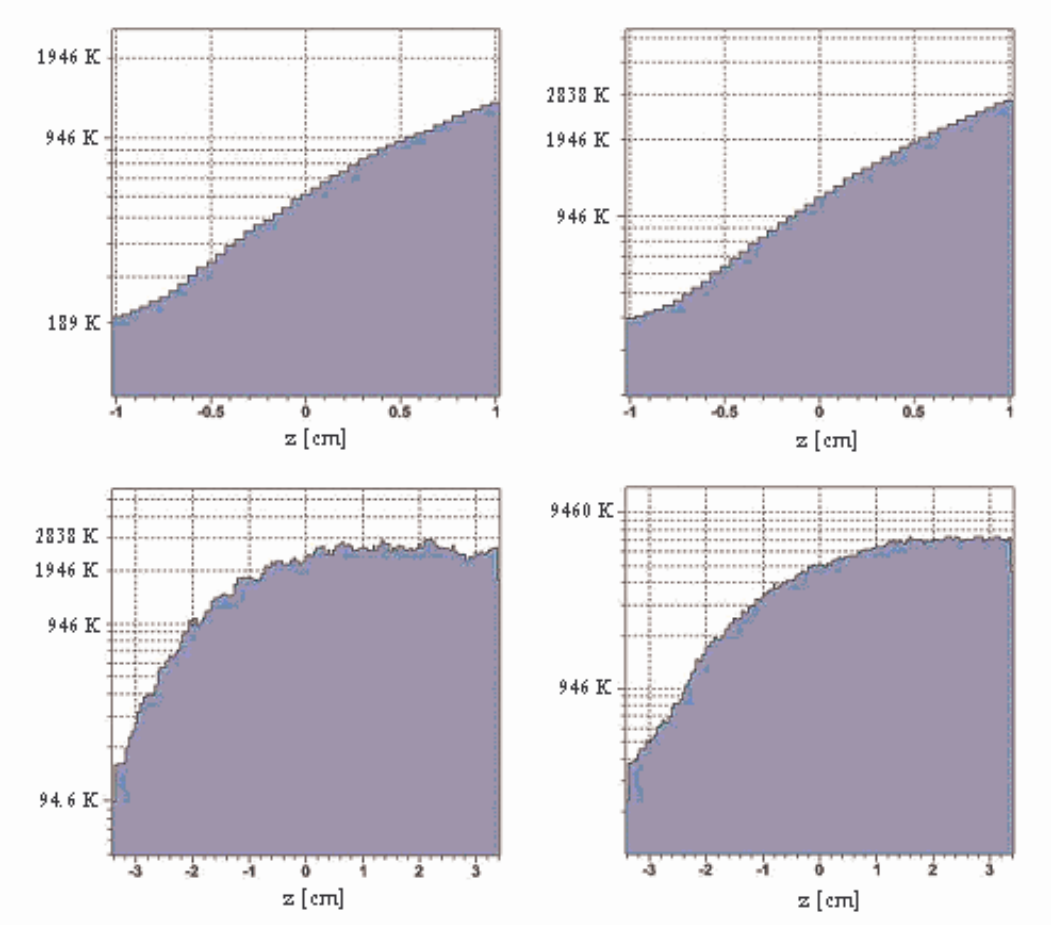

Figure 7. Temperature rises for a full Cu spoiler.

2.2 Metal and graphite options

The basic idea for these different alloy and graphite options is to have essentially a constant 0.6 radiation lengths of metal presented to the beam, regardless of the depth into the spoiler at which the beam enters. Therefore, there should not be a large difference in maximum temperature increase when comparing the two different cases that are being simulated: the bunch entering at 2 mm from the top (parallel to z axis) and the bunch hitting at 10 mm from

the top of the spoiler (parallel to z axis). Three different options are summarized in the following sections

2.2.1 Alloy and graphite option 1

This first option consists of a 0.6 radiation lengths middle block made of titanium alloy with leading and trailing taper made of graphite, covered by a 1mm thick layer of thick titanium alloy. Figure 8 shows a drawing of the spoiler. The dimensions are the same as for the full titanium alloy case.

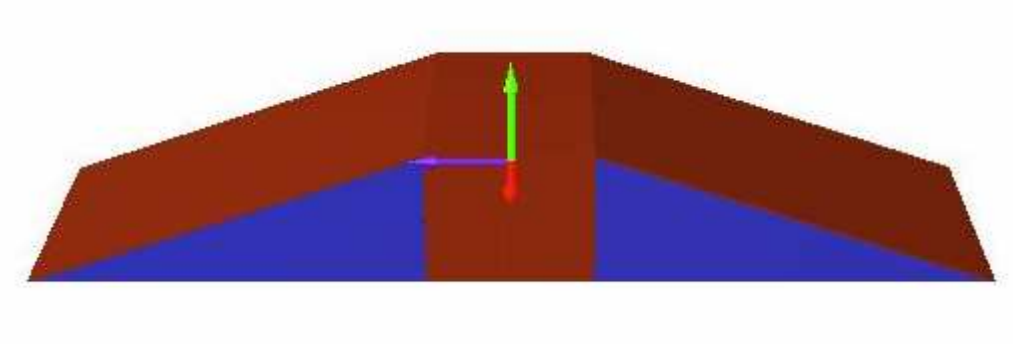

Figure 8. Ti alloy and graphite configuration option 1 spoiler.

In figure 9 are shown the temperature increase profiles along the beam axis, z, after the hit of one bunch. The green areas give the temperature profile in the graphite. The blue area is the temperature profile in the alloy. The scale of temperature at the left is only valid for the alloy area. The temperatures achieved at the graphite are given separately. The plots show how the particle shower is mainly generated in the metal region while the temperature increase at the graphite is quite constant. A slight shower in graphite can be observed in both 10 mm from the top cases, at the leading taper region.

Increases of temperature in the metal are more moderate than in the full metal spoiler, as expected. There is less material to generate a bigger shower of particles thus less energy is deposited in the alloy. Notice the peaks of temperature at the edges of both bottom plots, representing the increase of temperature at the layers on the tapers. Table 4 lists maximum temperature increases for this spoiler option. Only in the 500 GeV energy 10 mm from top case fracture temperature is reached.

Table 4. Top temperatures in all four cases for combination of Ti alloy and graphite option 1 spoiler.

	ΔT [K]; 250 GeV e^-	ΔT [K]; 500 GeV e^-
2 mm from top	325	640
10 mm from top	380	760
Difference	17%	19%

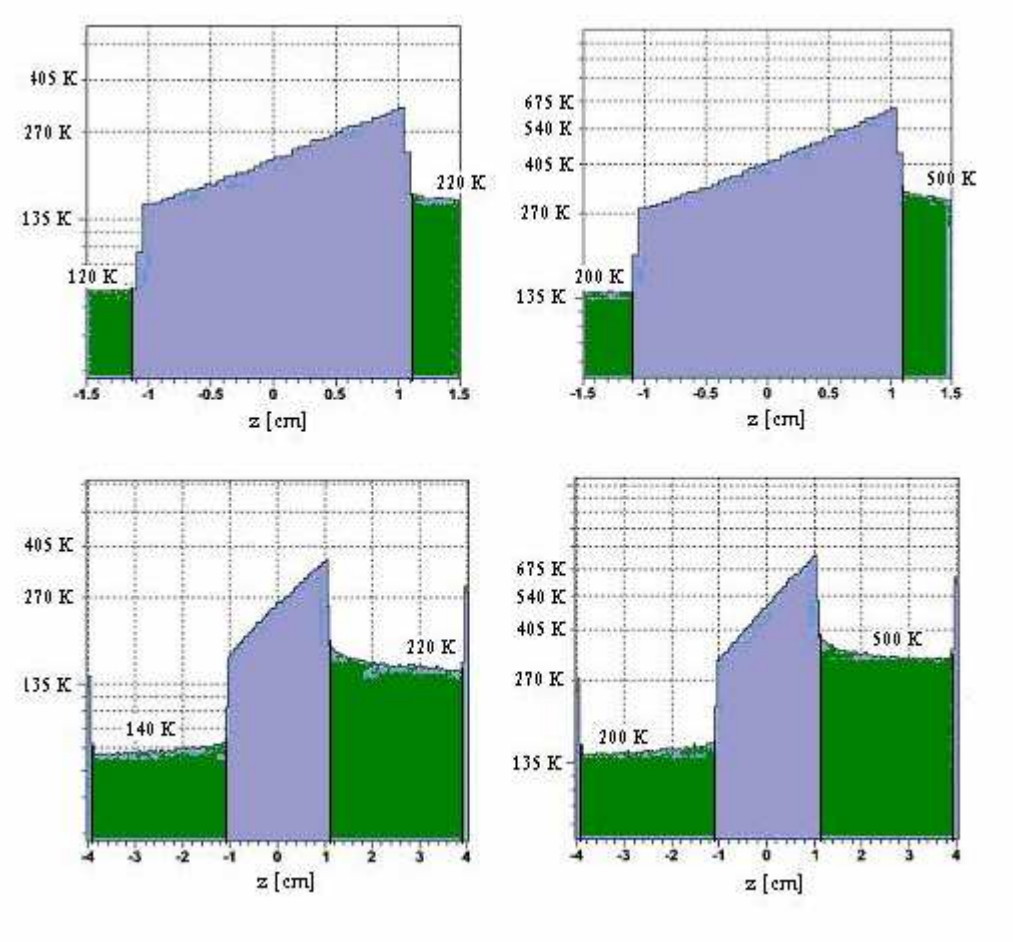

Figure 9. Temperature rises for combination option 1 of Ti alloy and graphite spoiler.

2.2.2 Alloy and graphite option 2

For this option the 0.6 radiation length of alloy are located mainly at the leading taper (figure 10), so when the bunch impacts the spoiler it will encounter first the main thickness of metal rather than the graphite. A 1 mm thick alloy layer is over the graphite at the trailing taper to ensure good electrical conductibility along the spoiler.

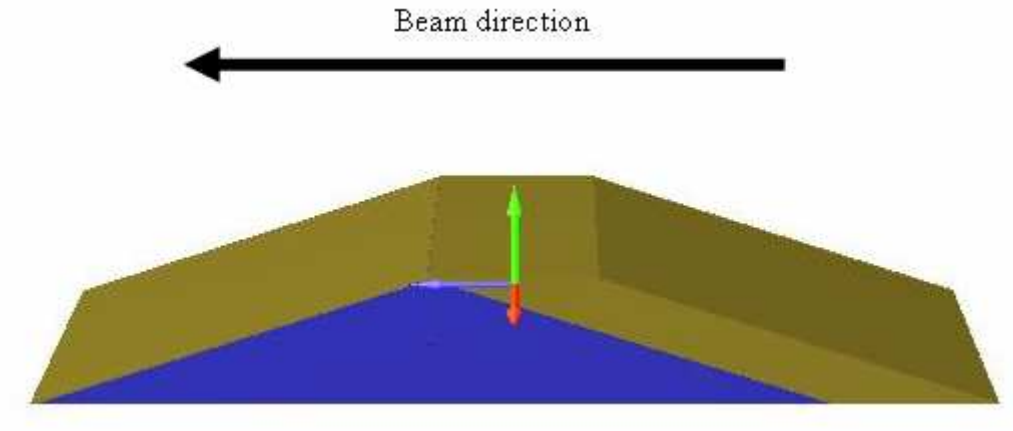

Figure 10. Ti alloy and graphite configuration option 2 spoiler.

Figure 11 shows the temperature increase profiles for that option. Again, the green area refers to the graphite while the blue refers to the alloy, and the left temperature axis of the plot is valid only for the alloy.

Table 5 lists the top temperatures for all the cases. These are the most moderate increases found with any of the options using titanium alloy. One of the most interesting aspects here is that there is essentially no dependence of the temperature rise on the position in which the beam traverses the spoiler. Another strong point with this option is that the increases of temperature are not enough to reach any dangerous temperature.

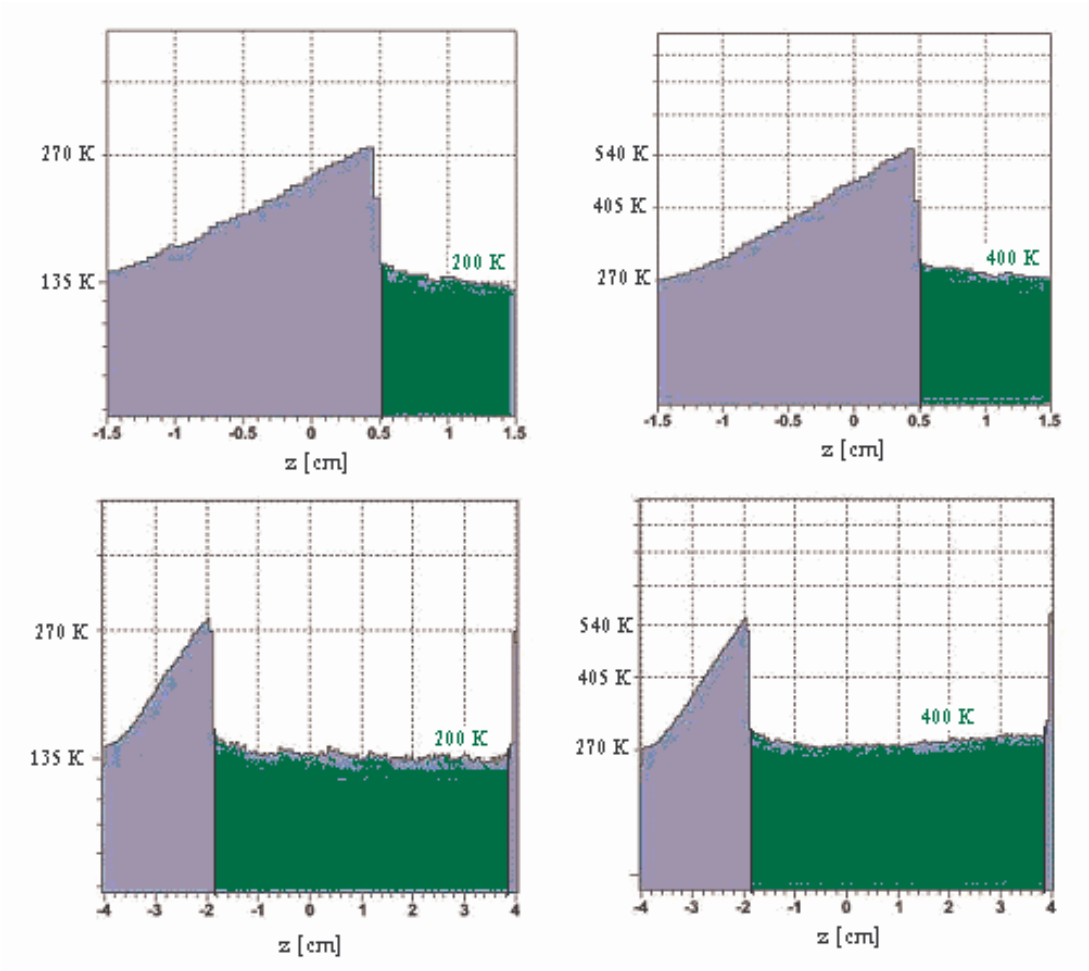

Figure 11. Temperature rises for combination option 2 of Ti alloy and graphite spoiler.

Table 5. Top temperatures in all four cases for combination of Ti alloy and graphite option 2 spoiler.

	ΔT [K]; 250 GeV e^-	ΔT [K]; 500 GeV e^-
2 mm from top	290	575
10 mm from top	295	580
Difference	2%	1%

2.2.3 Alloy and graphite option 3

The idea for this third option is the same as the others, to have a 0.6 radiation lengths of titanium alloy regardless of the beam position, but with the addition of the symmetric configuration that could simplify its manufacture. Figure 12 shows the drawing for this option.

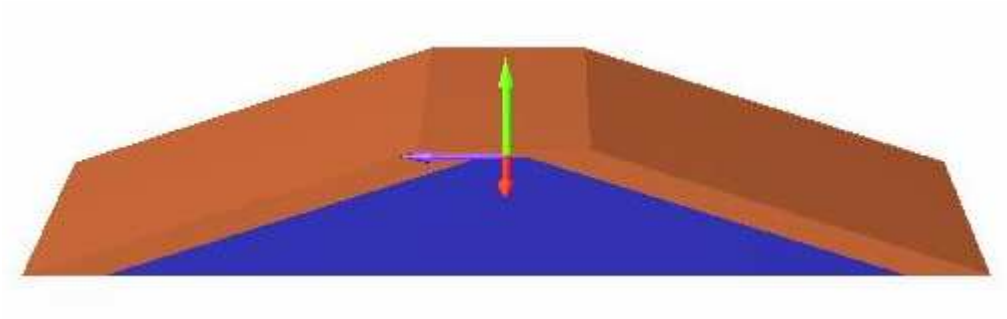

Figure 12. Ti alloy and graphite configuration option 3 spoiler.

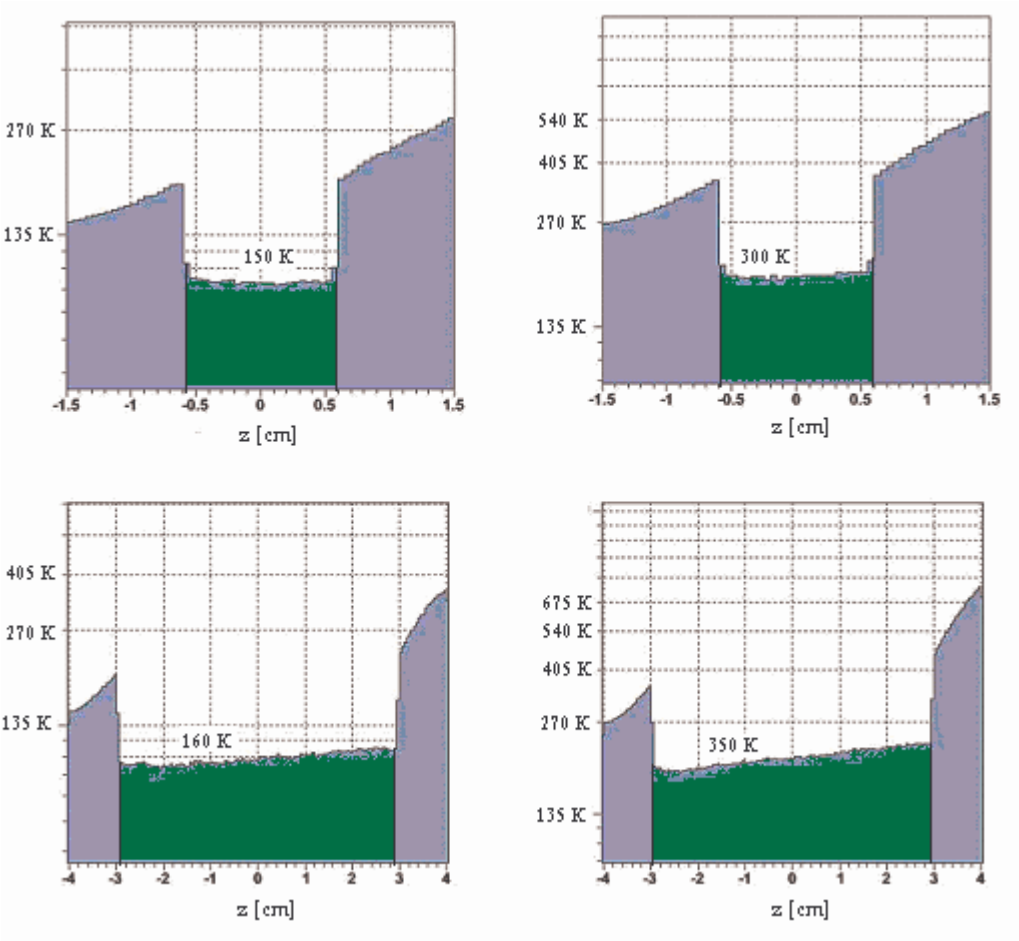

Figure 13. Temperature rises for combination option 3 of Ti alloy and graphite spoiler.

Again, the plots in figure 13 show the temperature increase profiles for the four different cases with the graphite and alloy zones as in figures 9 and 11. Table 6 lists the top temperatures and it can be observed that fracture temperature is reached for the 500 GeV energy 10 mm from the top case.

Table 6. Top temperatures in all four cases for combination of Ti alloy and graphite option 3 spoiler.

	ΔT [K]; 250 GeV e^-	ΔT [K]; 500 GeV e^-
2 mm from top	300	580
10 mm from top	370	760
Difference	23%	31%

2.2.4 Aluminium and graphite in the option 2 configuration

Simulations of this second configuration of metal and graphite were also done with aluminium and copper (see section 2.2.5). Figure 14 shows a picture of the spoiler, aluminium in grey, graphite in blue; and figure 15 the top temperature increases along the beam axis, with the blue area representing the aluminium and the green area the temperature increases in the graphite, the temperature axis being valid only for the aluminium. Table 7 shows the peak temperatures reached for this aluminium-graphite configuration and it can be observed that fracture will occur in all cases (considering that the spoiler is working in laboratory temperature conditions).

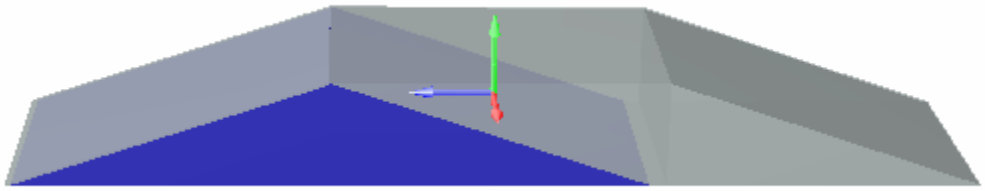

Fig. 14. Al and graphite configuration option 2 spoiler.

Table 7. Top temperatures in all four cases for combination of Al and graphite option 2 spoiler.

	ΔT [K]; 250 GeV e^-	ΔT [K]; 500 GeV e^-
2 mm from top	170	350
10 mm from top	175	370
Difference	3%	6%

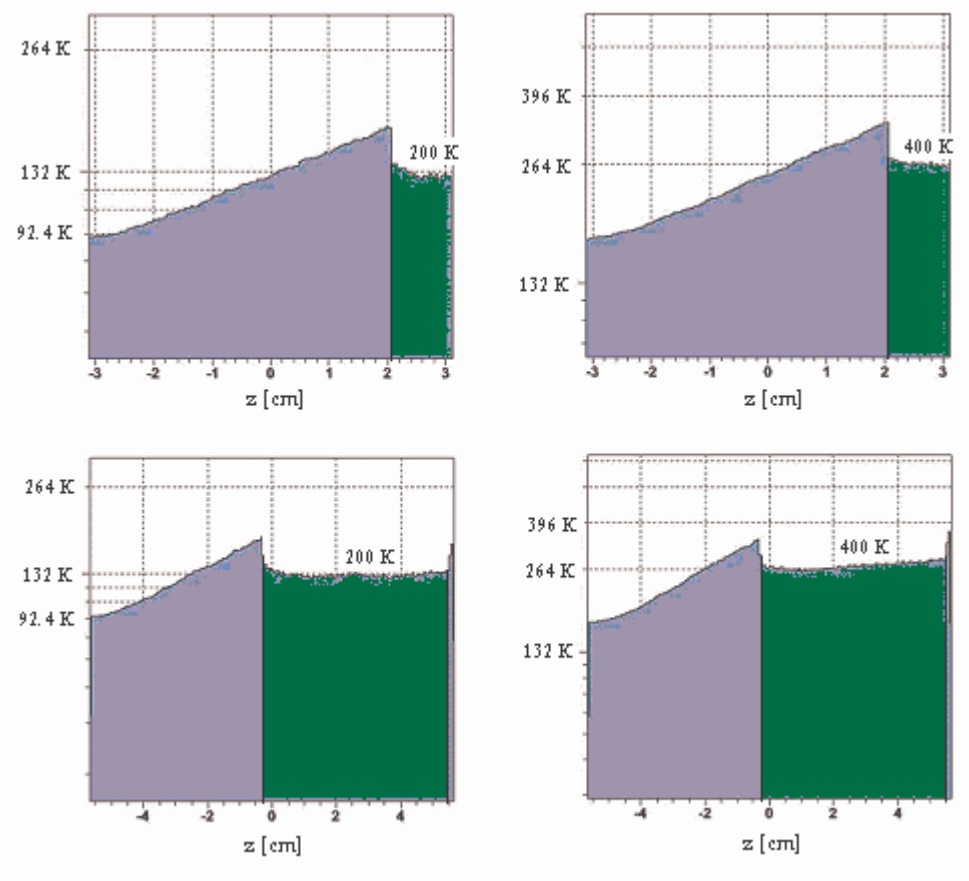

Fig. 15. Temperature rises for combination option 2 of Al and graphite spoiler.

2.2.5 Copper and graphite option 2

Figure 16 shows a picture of the spoiler, copper in red, graphite in blue; and figure 17 the top temperature increases along the beam axis, with the blue area representing the copper and the green area the temperature increases in the graphite, the temperature axis being valid only for the copper. Table 8 shows the top temperatures reached for this copper-graphite configuration.

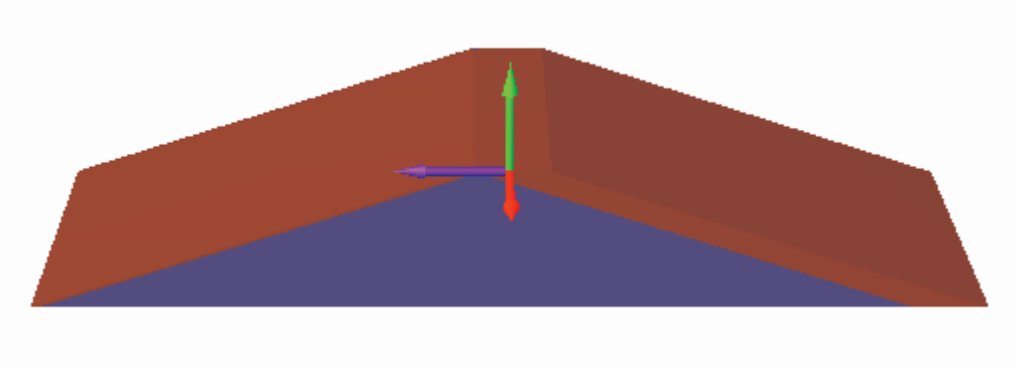

Fig. 16. Cu and graphite configuration option 2 spoiler.

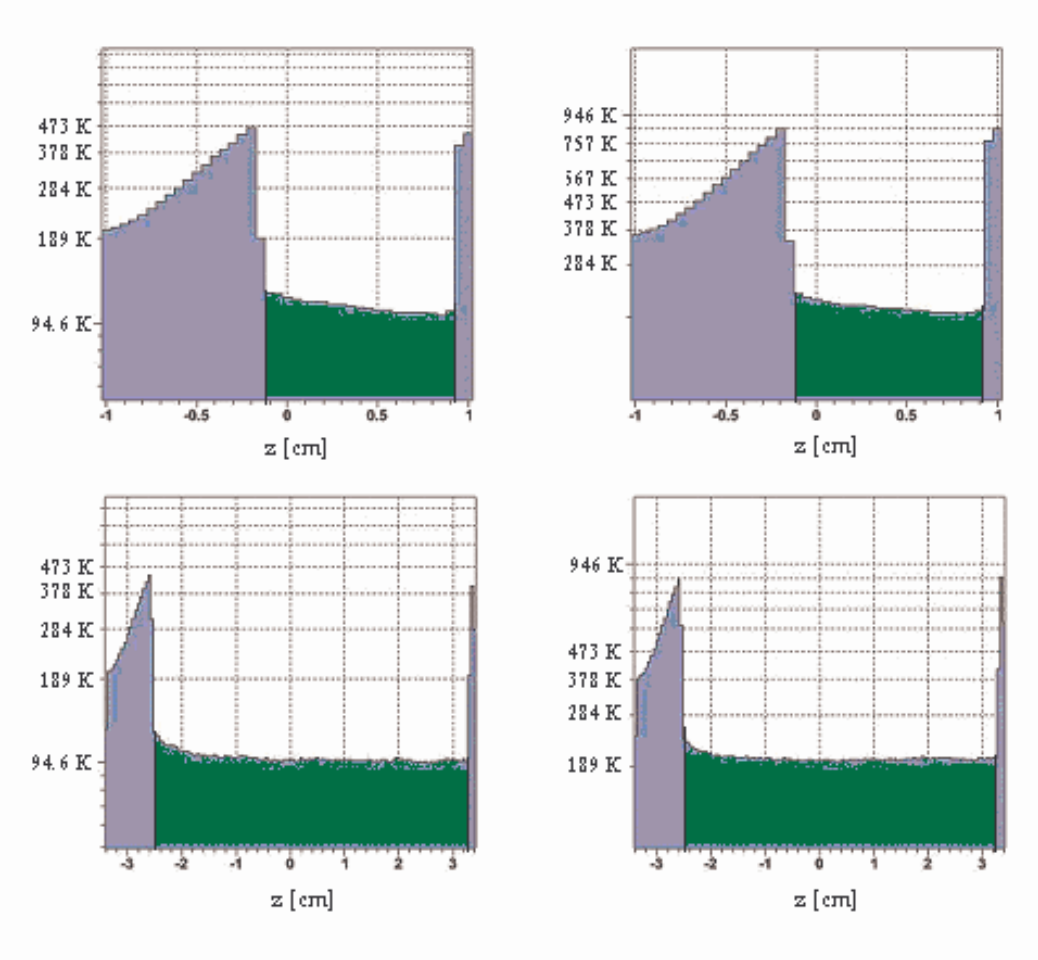

Fig. 17. Temperature rises for combination option 2 of Cu and graphite spoiler.

Table 8. Top temperatures in all four cases for combination of Cu and graphite option 2 spoiler.

	ΔT [K]; 250 GeV e^-	ΔT [K]; 500 GeV e^-
2 mm from top	465	860
10 mm from top	440	870
Difference	-5%	1%

For this configuration, when using copper, maximum increases of temperature do not reach values high enough to melt the metal, although the maximum temperatures reached in all four cases are enough to fracture or crack the material.

3 Summary and comparison of all the options

Table 9 summarises the maximum temperature increases for the four scenarios of beam energy and impact position, for each of the eight different geometry/material configurations considered so far.

It can be observed that the full metal spoilers are particularly prone to melting: in the case of the full copper spoiler this happens in all four scenarios and for the titanium and aluminium spoiler melting temperature is reached when the electrons of the bunch have an energy of 500 GeV and it traverses the spoiler 10 mm from the top. Problems with fracture are also observed in two cases for the titanium spoiler, 250 GeV of energy at 10 mm from the top and 500 GeV of energy 2 mm from the top and for all the different cases of Aluminium.

From the three different configurations of metal and graphite the one which gave best results is option 2. The option 2 geometry using titanium is predicted not to reach any fracture or melting temperature, whereas with aluminium it may reach fracture temperature in all cases. For copper, the fracture temperature is reached in all four cases. The other graphite-metal options, option 1 and 3, simulated only with titanium, show that fracture temperature is reached in the 500 GeV 10 mm from the top case.

Table 9. Summary of top temperatures reached in all the simulated spoilers.

	250 GeV e- 111x9 µm 2 mm from top	500 GeV e- 79.5x6.36 µm 2 mm from top	250 GeV e- 111x9 µm 10 mm from top	500 GeV e- 79.5x6.36 µm 2 mm from top
Full Ti alloy	420 K	870 K	850 K	2000 K
Full Al	200 K	210 K	265 K	595 K
Full Cu	1300 K	2700 K	2800 K	7000 K
Graphite+Ti option 1	325 K	640 K	380 K	760 K
Graphite+Ti option 2	290 K	575 K	295 K	580 K
Graphite+Ti option 3	300 K	580 K	370 K	760 K
Graphite+Al option 2	170 K	350 K	175 K	370 K
Graphite+Cu option 2	465 K	860 K	440 K	870 K

4 Conclusions

Increments of temperature differ of a factor two between 250 GeV and 500 GeV. This is almost entirely due to the factor of two difference in bunch area for both energies.

Simulations with copper have shown unacceptable results as either melting or fracture temperatures are reached in all the four different simulated cases. It is concluded that copper alone would be an inappropriate choice for the ILC collimators.

Aluminium options show the lowest temperature increases, but high enough to reach fracture temperature.

Graphite-metal configuration option 2 showed the best results, with the most moderate peak increases of temperatures. This is mainly due to the fact the bunch first encounters the bulk of the metal, before any electromagnetic shower has developed. This is in contrast to the other configurations where the bunch has traversed a significant amount of material prior to being incident on the metal, and therefore the metal is struck by a more substantially developed e.m. shower, consequently depositing more energy. Option 2 also shows no dependence in the bunch position, giving same results whether the bunch hit at 2 mm from the top of the spoiler or 10 mm from the top of it.

Titanium alloy-graphite configuration option 2 shows the most favourable results of any configuration considered, not reaching any melting or fracture temperatures, and deserves further consideration.

Acknowledgements

We acknowledge helpful discussions with colleagues, including J.Greenhalgh, G.Ellwood, R.J.Barlow, A.Bungau and L. Keller.

This work is supported by the Commission of the European Communities under the 6th Framework Programme “Structuring the European Research Area”, contract number RIDS-011899.

References

1. A.Fassò, A.Ferrari, P.R.Sala, "Electron-photon transport in FLUKA: status", Proceedings of the MonteCarlo 2000 Conference, Lisbon, October 23--26 2000, A.Kling, F.Barao, M.Nakagawa, L.Tavora, P.Vaz - eds., Springer-Verlag Berlin, p.159-164 (2001).
2. A.Fassò, A.Ferrari, J.Ranft, P.R.Sala, "FLUKA: Status and Prospective for Hadronic Applications", Proceedings of the MonteCarlo 2000 Conference, Lisbon, October 23-26 2000, A.Kling, F.Barao, M.Nakagawa, L.Tavora, P.Vaz - eds. , Springer-Verlag Berlin, p.955-960 (2001).
3. A.Bungau, R.J.Barlow *et al*., note in preparation.
4. G.Ellwood, J.Greenhalgh, note in preparation
5. Latest official version of ILC BCD for Beam Delivery System, http://www.linearcollider.org/wiki/lib/exe/fetch.php?cache=cache&media=bcd%3Av.12dec2005%3Abds.12dec2005.doc.
6. T-480 Collimator Wakefield Measurements, P.Tenenbaum, N.Watson *et al*., http://www-project.slac.stanford.edu/ilc/testfac/ESA/files/ColWake_TestBeamRequest.pdf
7. Specific choice of 0.6 radiation lengths and beam parameters are from ILC FF9 optics and L.Keller, http://www.astec.ac.uk/ap/collider/collimmeet02Nov05/keller_ILC_Errant_Bunches15.ppt
8. ILC Beam parameters, http://www-project.slac.stanford.edu/ilc/acceldev/beamparameters.html,
9. K-H. Buchegger, C.Theis, http://theis.home.cern.ch/theis/simplegeo/
10. A.Empl, http://www.fluka.org/tools/FlukaGUI.html